

Elevated expression of the membrane-anchored serine protease TMPRSS11E in NSCLC progression

Shufeng Li^{1*}, Zhenfa Chen¹, Wei Zhang¹, Ting Wang¹, Xihua Wang², Chao Wang¹, Jie Chao^{3,*}, Ling Liu^{4,*}

1 Key Laboratory of Developmental Genes and Human Disease in Ministry of Education, Jiangsu Provincial Key Laboratory of Critical Care Medicine, Department of Biochemistry and Molecular Biology, Medical School of Southeast University, Nanjing 210009, China

2. Department of respiration, Zhongda Hospital, Nanjing 210009, China.

3. Jiangsu Provincial Key Laboratory of Critical Care Medicine, Department of Physiology, Medical School of Southeast University, Nanjing 210009, China

4. Jiangsu Provincial Key Laboratory of Critical Care Medicine, Department of Critical Care Medicine, Zhongda Hospital, Medicine School of Southeast University, Nanjing, 210009, China

*Corresponding Author: Shufeng Li, Tel: 86-25-83272474; Fax: 86-25-83272500; Email: shufengli@seu.edu.cn

Ling Liu: liulingdoctor@126.com

Jie Chao: chaojie75@163.com

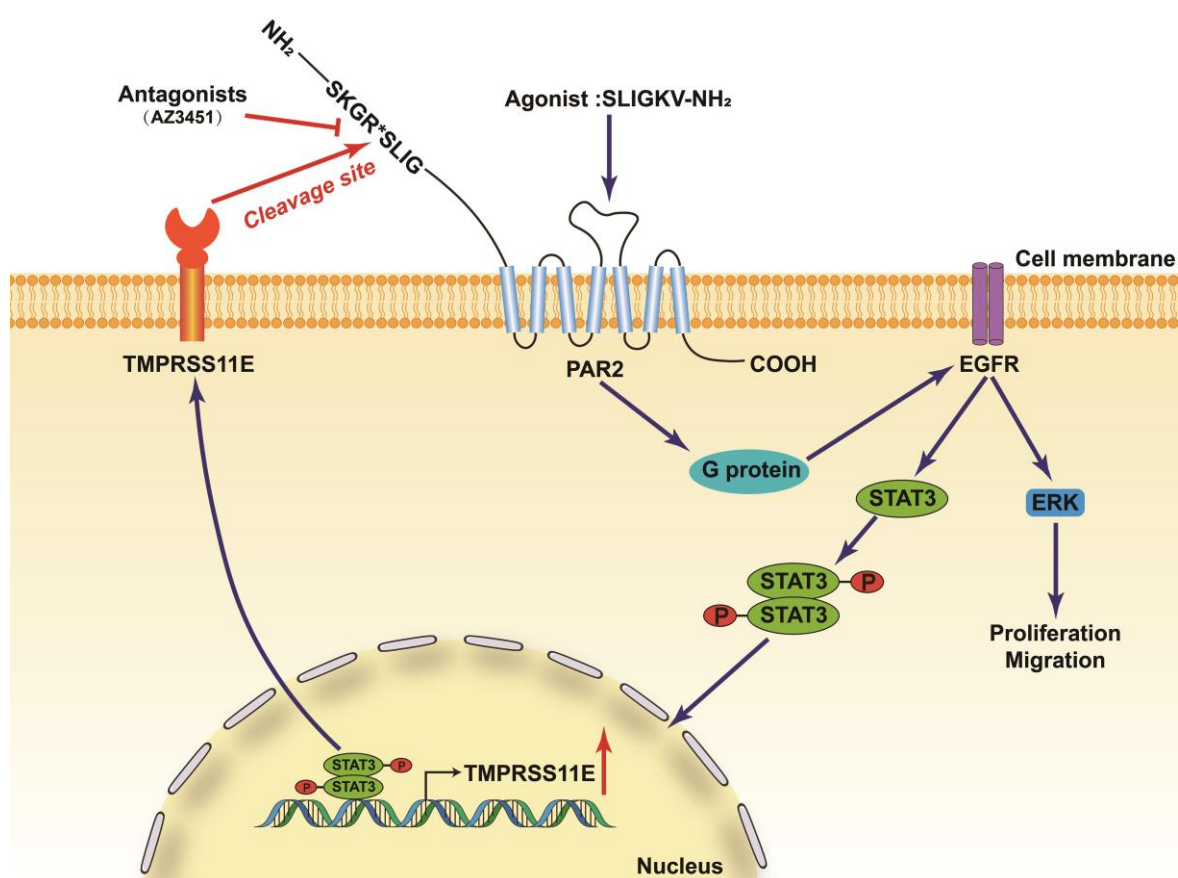
Abstract

TMPRSS11E was found to be upregulated in human non-small cell lung cancer samples (NSCLC) and cell lines, and high expression was associated with poor survival of NSCLC patients. The results of in vitro and in vivo experiments showed that overexpressing TMPRSS11E resulted in A549 cell proliferation and migration promotion, while the TMPRSS11E S372A mutant with the mutated catalytic domain lost the promoting function. In addition, in mouse xenograft models, silencing TMPRSS11E expression inhibited the growth of 95D cell-derived tumors. To explore the mechanism of marked upregulation of TMPRSS11E in NSCLC cells, promoter analysis, EMSA and ChIP assays were performed. STAT3 was identified as the transcription factor responsible for TMPRSS11E transcription. Moreover, the purified recombinant TMPRSS11E catalytic domain exhibited enzymatic activity for the proteolytic cleavage of PAR2. Recombinant TMPRSS11E catalytic domain incubation further activated the PAR2-EGFR-STAT3 pathway. These findings established a mechanism of TMPRSS11E-PAR2-EGFR-STAT3 positive feedback, and the oncogenic role of TMPRSS11E as a PAR2 modulator in NSCLC was revealed.

Key words:

TMPRSS11E, STAT3, protease activated receptor 2, transcription, NSCLC

Graphical Abstract



Accepted

Introduction

TMPRSS11E, also known as DESC1, belongs to the type II transmembrane serine protease (TTSP) family (1-2). Under normal physical conditions, TMPRSS11E and several HAT subfamily members of TTSP, are mainly expressed in squamous epithelium (3-5).

TMPRSS11E (DESC1) was first identified as a downregulated gene in squamous cell carcinoma of the head and neck (6). Later, in several cancers including ESCC, it was also found to be downregulated (7-10).

However, from our integrated analysis of six NSCLC gene expression datasets (GSE10072, GSE18842, GSE19804, GSE19188, GSE31552, and GSE101929), TMPRSS11E was identified as one of the 46 upregulated genes (11). Until now, the function of TMPRSS11E in NSCLC and the regulatory mechanism were still not known. Thus, in the current study, TMPRSS11E expression and activity in NSCLC were investigated. Our data revealed that upregulated TMPRSS11E played important roles in NSCLC progression; and that TMPRSS11E could be a biological marker of poor prognosis for NSCLC. Localized on the cell surface, TMPRSS11E functions as a proteolytic modifier of membrane PAR2 and plays a critical role in the activation of oncogenic signaling pathways.

Materials and methods

Specimens

This study included 50 clinical specimens (Supplementary Table S1). These human NSCLC tissues were collected from patients who underwent NSCLC resection at Zhongda Hospital (Nanjing, China) between January 2015 and May 2018. Informed consent was obtained from each patient, and the current study was approved by the Ethics Committee of Southeast University.

Cell culture, plasmids and reagents

The normal lung cell line BEAS-2B was from ATCC, HEK293, and the human NSCLC cell lines A549, H1299, PC9 and 95D were purchased from Shanghai Institute of Cell Biology, China (2017.04). The cells were cultured in DMEM supplemented with 10% fetal bovine serum (FBS) and 1% L-glutamine. All cell lines were routinely tested for bacterial and mycoplasma contamination and authenticated by short tandem repeat profiling (2021.06).

The plasmids used in this study are shown in Supplementary Table S2. The primers used for plasmid construction are listed in Supplementary Table S3. The antibodies and reagents used are shown in Supplementary Tables S4-S5.

qRT-PCR and Western blotting analysis

qRT-PCR and Western blotting were performed as previously described (12). The primers used for PCR are listed in Supplementary Table S3.

Chromatin immunoprecipitation (ChIP)

The ChIP assay was performed as reported previously (13). Briefly, after pCMV3-STAT3-FLAG transfection for 48 h, cells were crosslinked and then lysed and sonicated. Cell lysates were incubated with anti-STAT3 overnight, followed by addition of protein G beads.

Immunoprecipitated DNA was extracted, and PCR was performed to detect the amount of TMPRSS11E promoter. The primers used are listed in Supplementary Table S3.

Electrophoretic mobility shift assay (EMSA)

EMSA and supershift assays were performed using a LightShift™ Chemiluminescent EMSA Kit (13). Nuclear extracts from pCMV3-STAT3-FLAG-transfected cells were prepared. The regulatory sequences containing the STAT3-binding site in the TMPRSS11E promoter were synthesized, biotin-labeled and annealed as probes. Then, DNA-protein-binding reactions were subjected to nondenaturing polyacrylamide gel electrophoresis, transferred to

membranes, and detected by chemiluminescence. Probe sequences are shown in Supplementary Table S3.

Cell Counting Kit-8 Assay (CCK-8)

Cell proliferation was determined. Briefly, after transfection for 24h, the cells were seeded in a 96-well plate at a density of 2×10^3 cells per well and incubated for the indicated time (0-72h). Then, cell proliferation was evaluated using a CCK-8 kit. CCK-8 solution was added and incubated for 2 h at 37°C, and the absorbance value at 450 nm was measured. All assays were performed in triplicate and independently repeated three times.

Colony formation assay

Forty-eight hours after transfection, the cells were seeded into culture plates (60 mm) and cultured for 2 weeks. Cells were then fixed in ice-cold 70% methanol for 15 min and stained with Giemsa solution. Finally, colonies were photographed and counted.

Wound-healing assay

After transfection, the cells were cultured to confluence. Then, the cell layer was scratched using a pipette tip, and the scratched cells were washed and removed. Photographs were taken immediately after making the scratch, and after 48 h of culture, the area covered by migrated cells was calculated.

Transwell assays

After plasmid transfection for 12 hours, 1×10^5 cells in 200 μ l of serum-free medium were added to the upper chamber of the Transwell inserts, and 500 μ l of 20% FBS medium was added to the lower chamber. After incubation for 48 hours, the migrated cells attached to the lower surface were fixed and stained. Images were captured.

Subcutaneous tumor model

Nude mice (6 weeks of age) were obtained from Shanghai Laboratory Animal Center (Shanghai, China). Animal welfare and experimental procedures were performed strictly in accordance with high standard animal welfare and other related ethical regulations approved by Southeast University. Briefly, 1×10^6 cells were injected subcutaneously into the flanks of mice. Once tumors reached sizes of 5×5 mm, the mice were randomly assigned to different groups. TMPRSS11E-expressing plasmid or shRNA or control plasmid was complexed with GenEscortIII PEI and injected into the tumor, and the injection was repeated every 4 days for 4 cycles. The tumor volume was measured every 3 days. Finally, the mice were sacrificed, and the tumors were collected and weighed.

Luciferase reporter assay

Cells were seeded in 12-well plates and transfected with TMPRSS11E promoter luciferase constructs and 100 ng internal control plasmid pRSV- β -galactosidase. After transfection for 48 h, the cells were lysed, and luciferase activity was examined.

Expression of recombinant TMPRSS11E serine proteolytic domain (re-SP)

The catalytic domain of the TMPRSS11E-expressing plasmid was constructed and transformed into BL21(DE3). After IPTG induction, the cells were harvested and ultrasonicated. Then, by centrifugation, the supernatants and pellets were separated and analyzed by SDS-PAGE. Recombinant proteins were found mainly present in inclusion bodies (14). Next, inclusion bodies were washed and solubilized with 8 M urea, refolded by dialysis and stored at -20°C .

Internally quenched fluorescent (IQF) peptide substrate studies

Abz IQF peptides with the Tyr (3-NO₂) quenching group ([Abz-SKGRSLIG-Y(3-NO₂)], which was the PAR2 activation sequence, were synthesized. Hydrolysis of the PAR2 IQF peptide by re-SP was determined, and released fluorescence was monitored using a

Varioskan LUX microplate reader (Thermo Fisher) (2). The enzymatic reaction was performed in a final volume of 100 μ L in 100 mM Tris/HCl (pH 8.5). The cleavage site of IQF peptides by re-SP or trypsin was confirmed by MS analysis. To determine the Michaelis constant (K_m), different concentrations of peptides (0–400 μ M) were incubated with 5 nM re-SP for 15 min. Standard curves were obtained using the signal from the N-terminal Abz-containing cleavage fragment (Abz-SKGR) and were converted to molar concentrations of hydrolyzed product. Using the Lineweaver-Burk method of linearizing substrate-velocity data, K_m was determined.

Statistical methods

Data are presented as the mean \pm SEM of triplicate experiments. The statistical analysis involving two groups was performed using Student's *t* test. $P < 0.05$ was considered significant.

Results

TMPRSS11E expression was upregulated in NSCLC samples

In our previous research, through integrated analysis of six NSCLC gene expression datasets (GSE10072, GSE18842, GSE19804, GSE19188, GSE31552, and GSE101929), TMPRSS11E was found to be upregulated in all of these Gene Expression Omnibus datasets (8). To further explore the expression and significance of TMPRSS11E in NSCLC, first, TMPRSS11E expression was examined in 50 NSCLC tissue samples and the corresponding adjacent tissues collected at Zhongda Hospital. The qRT-PCR and Western blotting results showed that both the mRNA and protein levels of TMPRSS11E were markedly elevated in NSCLC tissues compared with paired nontumor tissues (Fig.1 A1-A2). Fig.1A3 shows the schematic structure of the TMPRSS11E protein. Fig.1A4 shows the representative Western blot results of TMPRSS11E expression in tumor tissues. As a protease, a prominent band with the molecular mass roughly expected for the zymogen form (48 kD) was observed (Fig.

1A4). In addition, activation products were also detected (28 kD). Next, the correlations between the TMPRSS11E expression level and clinicopathologic parameters were analyzed. The results showed that TMPRSS11E overexpression was closely correlated with tumor stage and tumor size ($P < 0.05$ for both, Supplementary Table S1). Importantly, the three-year cumulative survival rates of patients with high TMPRSS11E expression were significantly lower than those with low TMPRSS11E expression (Fig. 1A5). Our findings were consistent with TCGA data (Fig. 1B1-B2). All of these results indicated that TMPRSS11E expression levels were significantly upregulated in NSCLC tissues.

Activation of TMPRSS11E

For serine proteases, zymogen activation is essential for biological function. The activation of TMPRSS11E requires proteolytic cleavage at a canonical activation motif that converts the enzyme from a one-chain zymogen to an active, two-chain protease. Although activation cleavage of TMPRSS11E was observed in transfected cells (15) and in lung tissue, activation cleavage of TMPRSS11E was detected (Fig. 1A4). However, the responsible proteases (TMPRSS11E itself or other unknown proteases) and the location of the cleavage (intracellular or cell surface) are not clear. Therefore, activation cleavage of human TMPRSS11E in HEK293 cells was examined next. Plasmids expressing wild-type full-length TMPRSS11E (pCMV3-TMPRSS11E-FLAG) and a catalytically inactive mutant (pCMV3-TMPRSS11E-S372A-FLAG), which contains an alanine instead of serine in the active center (amino acid 372), were constructed. After transfection and Western blot analysis, the results showed that no activation cleavage was detected in cells transfected with the catalytically inactive mutant S372A (Fig. 2A), which indicated that TMPRSS11E activation can be mediated by autocatalysis. For further characterization of human TMPRSS11E, a plasmid expressing fusion proteins of the wild-type serine proteinase domain (SP) with a FLAG tag (pet28-SP) was constructed (Fig. 2B). Recombinant SP was expressed in bacteria and was

almost exclusively expressed as inclusion bodies. After solubilization and renaturation, the soluble refolded re-SP was analyzed by SDS-PAGE followed by Coomassie staining (Fig. 2C). The SDS-PAGE result confirmed the good quality of our material, and the yielded re-SP was then used for the following research. When HEK293 cells were transfected with the catalytically inactive mutant plasmid pCMV3-TMPRSS11E-S372A-FLAG, re-SP protein incubation was followed, and Western blot analysis showed that re-SP protein could cleave the TMPRSS11E mutant S372A, as shown in Fig. 2D. These data indicated that no other endogenous proteases were capable of cleaving TMPRSS11E in HEK293 cells. Moreover, Fig. 2E shows that trypsin exposure also resulted in more SP formation in wild-type TMPRSS11E-transfected cells, and the TMPRSS11E mutant S372A could also be cleaved by trypsin, as evidenced by the appearance of the prominent 28 kD band under reducing conditions. In summary, this analysis showed that TMPRSS11E was expressed as a precursor or zymogen form that may be activated by pericellular trypsin or by autoactivation by itself. To the best of our knowledge, trypsin is the first exogenous enzyme proven to activate TMPRSS11E.

In vitro and in vivo effects of TMPRSS11E overexpression on NSCLC progression

To explore the expression and significance of TMPRSS11E in NSCLC cell lines, we first measured the endogenous expression levels of TMPRSS11E in the normal lung cell line BEAS-2B and four NSCLC cell lines using qRT-PCR and Western blotting. The results showed that TMPRSS11E expression was upregulated in NSCLC cells compared with the normal lung cell line BEAS-2B (Fig. 3A1-3A2). Furthermore, CCK-8 and colony formation assays showed that cell proliferation was significantly increased in the TMPRSS11E overexpression group (Fig. 3B-3C). In addition, the Transwell migration assays and in vitro scratch wound healing assays indicated that TMPRSS11E overexpression significantly enhanced cell migration (Fig. 3D-3E). Furthermore, we investigated the importance of

protease activity for its function in NSCLC. With the TMPRSS11E S372A mutant, which abolished the catalytic function overexpressed in A549 cells, the promoting activity was lost, as demonstrated by the CCK-8, colony formation, Transwell and wound healing assays (Fig. 3B-3E). Then, in vivo experiments further confirmed that TMPRSS11E overexpression resulted in an increase in tumor growth compared with that in the control group. Furthermore, the increase in tumor growth was eliminated when the TMPRSS11E S372A mutant was expressed (Fig. 4A1-4A4). These results indicated that the upregulation of TMPRSS11E could promote NSCLC cell progression in vitro and in vivo. The increased growth events caused by TMPRSS11E were abolished when the catalytic function was lost, suggesting that the cleavage activity of TMPRSS11E was crucial for its function.

TMPRSS11E knockdown inhibited tumor growth in vivo

Upregulation of TMPRSS11E in lung tumors suggested that these enzymes were important for tumor development and may therefore be potential targets for NSCLC therapy. To inhibit endogenous high TMPRSS11E levels, 95D cell lines were transfected with control short hairpin RNA (shCtrl) or TMPRSS11E-specific shRNA- expressing plasmids, and the results showed that shTMPRSS11E2# and shTMPRSS11E3# could greatly decrease the level of TMPRSS11E mRNA and protein expression in NSCLC cells; thus, shTMPRSS11E 2# and 3# were selected and used for further experiments (Fig. 4B1-4B2). In vivo experiments were performed to examine whether TMPRSS11E-specific shRNA treatment could decrease tumor growth, and PEI-complexed shTMPRSS11E 2# or 3# was injected into the tumors of nude mice. The results revealed that both groups receiving either TMPRSS11E-specific shRNA expression plasmid treatment showed decreases in tumor size and weight compared with the control group (Fig. 4C1-4C3). These results confirmed the protumorigenic role of TMPRSS11E in NSCLC progression.

STAT3 mediated TMPRSS11E transcription.

To further explore the mechanisms underlying the upregulation of TMPRSS11E in NSCLC, the promoter region was analyzed, and two STAT3-binding sites were predicted by PROMO (Fig. 5A). To determine whether STAT3 could contribute to the transcriptional regulation of the TMPRSS11E gene, TMPRSS11E promoter reporter plasmids were constructed (Fig. 5B). TMPRSS11E promoter reporter plasmids and pRSV- β -galactosidase control plasmids were cotransfected into A549 and 95D cells, and the luciferase activity in the cell extracts was measured and is shown in Fig. 5B. Mutations at distal STAT3 binding site A in P-900mA/+15-luc or truncated P-540/+15-luc without site A both had a decreased effect on TMPRSS11E promoter activity compared with P-900/+15-luc, indicating that site A contributes to transcriptional activity. In addition, the truncated plasmid p-520/+15-luc compared with p-540/+15-luc containing proximal STAT3-binding site B had a significant reduction in promoter activity, indicating that site B also contributed to transcriptional activity. Consistent with these results, overexpression of STAT3 or STAT3C failed to stimulate promoter activity of p-520/+15-luc without STAT3-binding sites A and B, but both STAT3 and STAT3C (constitutively activated STAT3) overexpression could still activate the promoter activity of the reporter plasmid with a single B site, and the activity of the plasmid with both A and B sites was more activated compared with the control group in A549 and 95D cells (Fig. 5C-5D). Moreover, STAT3- or STAT3C- overexpressing plasmid transfection both enhanced TMPRSS11E expression in A549 and 95D cells (Fig. 5E). In addition, the STAT3 inhibitor BP-1-102 reversed the increase in TMPRSS11E levels induced by STAT3 overexpression in NSCLC cells A549 and 95D (Fig. 5F). TMPRSS11E decreased in a dose-dependent manner with the STAT3 inhibitor BP-1-102.

To further test whether STAT3 could bind to the region of the TMPRSS11E promoter via the putative binding sites, EMSA and ChIP assays were performed. As shown in Fig. 5G, DNA–

protein complexes were detected when the nuclear extracts of A549 or 95D cells were incubated with probes containing STAT3-binding site A or site B. The DNA–protein complex was prevented in competition experiments, and the specificity was also confirmed by a supershift assay with an anti-STAT3 antibody. In addition, ChIP assays demonstrated that STAT3 was recruited to the TMPRSS11E promoter, as shown in Fig. 5H. More interestingly, RNA-Seq data from GSE100399 showed that compared with wild-type animals, STAT3 knockdown markedly reduced TMPRSS11E expression in cutaneous squamous cell carcinoma cells,

(<https://www.ncbi.nlm.nih.gov/geo/query/acc.cgi?acc=GSE100399>). These data agreed with our results. Taken together, these findings strongly suggested that STAT3 is responsible for the transcription of TMPRSS11E. Indeed, a high level of phosphorylated STAT3 was a predictor of poor prognosis in NSCLC (16-17)

TMPRSS11E triggers the EGFR pathway through activation of PAR2

Next, we investigated the potential substrate of TMPRSS11E and determined how elevated TMPRSS11E affects NSCLC cell proliferation and migration. As a feature of serine proteases, the protease domain of TMPRSS11E was characterized by a triad of His, Asp, and Ser residues that are necessary for catalytic activity. According to the analysis of crystal structure, activated TMPRSS11E should efficiently hydrolyze peptide substrates containing P1-Arg (18). Human airway trypsin-like protease (HAT), a member of the HAT/DESC subfamily of TTSP, is involved in inflammation by activating PAR2 in several cell types (19-20). However, whether TMPRSS11E can activate PAR2 in NSCLC has not been reported.

PAR2 (protease-activated receptor 2) is also named F2RL1. It is a G protein-coupled receptor (GPCRs) that modulates a variety of downstream signaling pathways and cell functions in numerous cancer cells. TCGA data showed that PAR2 expression exhibited a notable

enhancement during NSCLC tumor progression, while there was a close correlation between PAR2 expression and the survival of NSCLC patients (Fig. 6A1-6A2). To analyze the capacity of TMPRSS11E for PAR2 cleavage, the recombinant SP was enzymatically further characterized. Internally quenched fluorescent (IQF) peptides with PAR2 N-terminal sequences that contain the known activation site [Abz-SKGRSLIG-Y(3-NO₂)] were synthesized (21). After incubation with re-SP, the released fluorescence was detected. The results showed that Abz-RQRRVVGG-Y(3-NO₂) was efficiently cleaved by TMPRSS11E (Fig. 6B1). Then, curves were plotted for the relative activity versus substance concentration. By calculation, the K_m value was determined to be 150 μM for the IQF peptides (Fig. 6B2). Importantly, a transactivation has been reported between PAR2 and EGFR in cancer cells, which potentiates PAR2 to modulate EGFR phosphorylation, cooperatively mediating cellular signaling, such as the ERK and STAT3 signaling pathways (22). As PAR2 is a substrate of TMPRSS11E, the influence of TMPRSS11E on the EGFR pathway in A549 and 95D cells was investigated. Similar to PAR2 agonist treatment, the addition of recombinant TMPRSS11E SP (10 μg/ml) to the medium significantly induced EGFR phosphorylation in A549 and 95D cells, as measured by Western blotting of phosphorylated tyrosine 1068 in EGFR (Fig. 6C). Because EGFR signaling acts mainly through the Raf/Mek/ERK and STAT3 pathways, these pathways in cells transiently exposed to TMPRSS11E were then examined. After the addition of recombinant TMPRSS11E SP (10 μg/ml) or PAR2 AP to the medium, STAT3 phosphorylation was notably elevated compared with that in control cells. In addition, the protease-activated receptor-2 (PAR2) antagonist AZ3451 reversed the phosphorylation level of EGFR or STAT3 increased by re-SP incubation in A549 and 95D cells (Fig. 6C). Taken together, transient re-SP exposure modified the PAR2-EGFR-STAT3 pathway. Our results suggested that TMPRSS11E promoted the PAR2-dependent transactivation of EGFR. Thus,

the PAR2-EGFR-STAT3 pathway could further induce more TMPRSS11E expression and form a positive feedback cycle.

Discussion

TMPRSS11E (DESC1) was first identified as a tumor suppressor gene in squamous cell carcinoma of the head and neck(3). However, overexpression of TMPRSS11E in a variety of carcinomas, such as kidney, brain and breast cancer, has also been reported (23). The present study reported the novel finding that TMPRSS11E was highly overexpressed in NSCLC and important for lung cancer development. We showed here the first evidence that TMPRSS11E was highly expressed in lung cancer cell lines and patients and that such expression was significantly associated with poor prognosis. Recent studies also showed that TMPRSS11E plays a protumorigenic role in some tumor types (23), but the mechanism of TMPRSS11E, which is involved in the progression of tumor cells, is not clear. The novelty of this study was as follows: first, to the best of our knowledge, this is the first study to demonstrate a contribution of TMPRSS11E during the progression of NSCLC. Second, STAT3 was demonstrated to contribute to the transcriptional regulation of the TMPRSS11E gene. Third, human TMPRSS11E zymogen could also be activated by trypsin on the cell surface. Finally, with the production and purification of the recombinant catalytic domain of this protease (re-SP), the function of TMPRSS11E in PAR2 activation was confirmed. Recently, PAR2 blockade was reported to sensitize gefitinib or osimertinib, which are commonly used EGFR-tyrosine kinase inhibitors (EGFR-TKIs), and reverse their resistance mainly via the EGFR-ERK signaling axis (24-25). Therefore, their report together with our work suggest that the proteinase TMPRSS11E, as a PAR2 regulator, is important for NSCLC. TMPRSS11E was also reported to participate in the degradation of ECM components such as fibronectin, gelatin and fibrinogen (23). Our results showed another function of TMPRSS11E as a modulator of PAR2 activation and signaling. Moreover, PAR2 was reported to signal to

various downstream pathways that modulate not only cell proliferation, migration and tumor development but also cytokine production and the inflammatory response (26). PAR2 is present in various kinds of cells, including airway epithelial cells (27), and is involved in inflammatory conditions, such as idiopathic pulmonary fibrosis and bronchial asthma. In inflamed lungs, human airway trypsin-like protease (HAT) displays its functions via PAR2 activation (28-29). Therefore, TMPRSS11E may also be involved in lung inflammation by PAR2 activation. In addition, TMPRSS11E is induced by STAT3, while STAT3 regulates both inflammation and tumors (30-31). In light of these findings, TMPRSS11E might not only promote NSCLC development but also be related to airway inflammatory diseases. These roles still need further investigation.

Overall, the role of many TTSP family members, including TMPRSS11E, in development, physiological function and cancer progression remains elusive. Deregulated expression of several TTSP members has been linked to various disorders, including anemia, osteoarthritis, cancer, skin defects, cardiovascular diseases and obesity (1). Each member appears to have diverse functions in normal tissues as well as in cancer progression. The physiological function of TMPRSS11E remains to be further investigated.

Funding

This study was supported by Grant from the Chinese National Nature Science Foundation (31070706).

Authors' Contributions

S.L designed the study and analyzed the data and wrote the manuscript. J.C. and L.L. analyzed the data and provided suggestions for the project. Z.C., W.Z. and T.W. performed the experiments. X.W. and C.W. collected the tissue samples and clinical data of patients. All authors have informed consent to the publication of this article.

Data availability statement

Data are available from the corresponding author upon reasonable request.

Conflict of Interest Statement

The authors declared that they have no conflict of interest.

References:

1. Murza, A. et al. (2020) Inhibitors of type II transmembrane serine proteases in the treatment of diseases of the respiratory tract - A review of patent literature. *Expert Opin Ther Pat.*, 30,807-824.
2. Béliveau, F. et al (2009) Probing the substrate specificities of matriptase, matriptase-2, hepsin and DESC1 with internally quenched fluorescent peptides. *FEBS J.*, 276, 2213-26.
3. Sales, K.U. et al. (2011) Expression and genetic loss of function analysis of the HAT/DESC cluster proteases TMPRSS11A and HAT. *PLoS One.* 6, e23261.
4. Ovaere, P. et al. (2009) The emerging roles of serine protease cascades in the epidermis. *Trends Biochem Sci.* 34, 453-63.
5. Zhang, Z. et al. (2017) The Transmembrane Serine Protease HAT-like 4 Is Important for Epidermal Barrier Function to Prevent Body Fluid Loss. *Sci Rep.* 7, 45262.
6. Lang, J.C. et al (2001) Differential expression of a novel serine protease homologue in squamous cell carcinoma of the head and neck. *Br J Cancer*, 84, 237-243
7. Sedghizadeh, P.P. et al (2006) Expression of the serine protease DESC1 correlates directly with normal keratinocyte differentiation and inversely with head and neck squamous cell carcinoma progression. *Head Neck*, 28, 432-40.
8. Uchikado, Y. et al. (2006) Gene expression profiling of lymph node metastasis by oligomicroarray analysis using laser microdissection in esophageal squamous cell carcinoma. *Int J Oncol.*, 29:1337–47.
9. Kashyap, M.K. et al. (2009) Genomewide mRNA profiling of esophageal squamous cell carcinoma for identification of cancer biomarkers. *Cancer Biol Ther.*, 8, 36–46.

10. Zinovyeva, M.V. et al. (2010) Identification of some human genes regulated during esophageal squamous cell carcinoma formation and human embryonic esophagus development. *Dis Esophagus*, 23, 260-70.
11. Li, M. et al. (2021) MALAT1 modulated FOXP3 ubiquitination then affected GINS1 transcription and driven NSCLC proliferation. *Oncogene*. 40, 3870-3884.
12. Li, S. et al. (2018) Long non-coding RNA metastasis-associated lung adenocarcinoma transcript 1 promotes lung adenocarcinoma by directly interacting with specificity protein 1. *Cancer Sci*. 109,1346-1356.
13. Li, S. et al (2015) Sp1-mediated transcriptional regulation of MALAT1 plays a critical role in tumor. *J Cancer Res Clin Oncol*. 141, 1909-20.
14. Behrens, M. et al. (2009) Substrate specificity of rat DESC4, a type II transmembrane serine protease. *Protein Pept Lett*. 16, 1-6.
15. Zmora, P. et al. (2018) TMPRSS11A activates the influenza A virus hemagglutinin and the MERS coronavirus spike protein and is insensitive against blockade by HAI-1. *J Biol Chem*. 293, 13863-13873.
16. Zheng, Q. et al. (2021) A novel STAT3 inhibitor W2014-S regresses human non-small cell lung cancer xenografts and sensitizes EGFR-TKI acquired resistance. *Theranostics*. 11, 824-840.
17. Parakh, S. et al. (2021) Multicellular Effects of STAT3 in Non-small Cell Lung Cancer: Mechanistic Insights and Therapeutic Opportunities. *Cancers (Basel)*. 13, 6228.
18. Kyrieleis, O.J. et al. (2007) Crystal structure of the catalytic domain of DESC1, a new member of the type II transmembrane serine proteinase family. *FEBS J*., 274, 2148-60.

19. Pawar, N.R. et al. (2019) Membrane-Anchored Serine Proteases and Protease-Activated Receptor-2-Mediated Signaling: Co-Conspirators in Cancer Progression. *Cancer Res.*, 79, 301-310.
20. Coelho, A.M. et al. (2003) Proteinase-activated receptor-2: physiological and pathophysiological roles. *Curr Med Chem Cardiovasc Hematol Agents*. 1, 61-72.
21. Kim, K.K. et al. (2020) Role of trypsin and protease-activated receptor-2 in ovarian cancer. *PLoS One*. 15, e0232253.
22. Jiang, Y. et al. (2021) PAR2 induces ovarian cancer cell motility by merging three signalling pathways to transactivate EGFR. *Br J Pharmacol*. 178, 913-932.
23. Vilorio, C.G. et al. (2007) Human DESC1 serine protease confers tumorigenic properties to MDCK cells and it is upregulated in tumours of different origin. *Br J Cancer*. 97, 201-9.
24. Jiang, Y. et al. (2021) Targeting PAR2 Overcomes Gefitinib Resistance in Non-Small-Cell Lung Cancer Cells Through Inhibition of EGFR Transactivation. *Front Pharmacol*. 12, 625289.
25. Jiang, Y. et al. (2022) PAR2 blockade reverses osimertinib resistance in non-small-cell lung cancer cells via attenuating ERK-mediated EMT and PD-L1 expression. *Biochim Biophys Acta Mol Cell Res*. 1869, 119144.
26. Dorsam, R.T. et al. (2007) G-protein-coupled receptors and cancer. *Nat Rev Cancer*. 7, 79-94.
27. Larsen, A.K. et al. (2008) Salmon trypsin stimulates the expression of interleukin-8 via protease-activated receptor-2. *Toxicol Appl Pharmacol*. 230, 276-82.

28. Miki, M. et al. (2019) Human airway trypsin-like protease enhances interleukin-8 synthesis in bronchial epithelial cells by activating protease-activated receptor 2. *Arch Biochem Biophys.* 664, 167-173.
29. Ostrowska, E. et al. (2007) PAR-2 activation and LPS synergistically enhance inflammatory signaling in airway epithelial cells by raising PAR expression level and interleukin-8 release. *Am J Physiol Lung Cell Mol Physiol.* 293, L1208-18.
30. Mohrherr, J. et al. (2020) STAT3: Versatile Functions in Non-Small Cell Lung Cancer. *Cancers (Basel).* 12, 1107.
31. Simeone-Penney, M.C. et al. (2007) Airway epithelial STAT3 is required for allergic inflammation in a murine model of asthma. *J Immunol.* 178, 6191-9.

Accepted Manuscript

Figure legend

Fig. 1. TMPRSS11E was upregulated in NSCLC. A. TMPRSS11E expression in 50 NSCLC tumors and peritumoral lung tissues. A1. qRT-PCR analysis. A2. Western blot analysis. Actin protein expression was used as an internal control. A3. Schematic representation of TMPRSS11E with catalytic residues highlighted. TM, transmembrane; SEA, sea urchin sperm protein, aggrecan, and enterokinase domain; SP, serine protease domain. Expected molecular masses for TMPRSS11E zymogen and the predicted cleaved protease domain (SP) are shown. A4. Representative Western blotting analysis of TMPRSS11E protein expression (T, tumor; N, nontumorous tissues). A5. Survival curves for 50 patients with NSCLC. B1. Expression of TMPRSS11E in LUAD or LUSC from TCGA data. (<http://ualcan.path.uab.edu/index.html>). LUAD: Lung adenocarcinoma, LUSC: Lung squamous cell carcinoma. T: tumor; N: normal tissues. B2. Survival curves of the TCGA NSCLC dataset.

Fig. 2. TMPRSS11E expression and cleavage in HEK293 cells. A. Western blotting of TMPRSS11E proteins in lysates from HEK293 cells transfected with TMPRSS11E or TMPRSS11E S372A mutant expressing plasmid. Experiments were performed under nonreducing or reducing conditions with anti-FLAG antibody. The full-length TMPRSS11E and the cleaved fragment are indicated by arrowheads. GAPDH was used as a protein loading control. Data are representative of at least three experiments. B. Schematic diagram of the recombinant TMPRSS11E protease domain (re-SP). Numbers indicate the first and last amino acids of the TMPRSS11E protease domain constructs. The recombinant TMPRSS11E protease domain contains a His6 epitope at the N-terminus and a flag epitope at the C-terminus. C. Expression of the recombinant TMPRSS11E protease domain in *E. coli*. SDS-PAGE analysis of the purified recombinant TMPRSS11E protease domain. D. Purified recombinant TMPRSS11E protease domain (re-SP) could cleave the TMPRSS11E S372A

mutant protein expressed in HEK293 cells. HEK293 cells transfected with plasmids expressing TMPRSS11E S372A mutant or control vector. After transfection for 48h, the cells were incubated with purified re-SP (10 µg) at 37 °C for 5 min. Western blotting was performed under reducing conditions with anti-FLAG antibody. E. Analysis of TMPRSS11E in HEK293 cells treated with trypsin. HEK293 cells expressing TMPRSS11E or the S372A mutant were treated with buffer (control) or trypsin (100 µg/ml) 5 minutes before being lysed for Western blotting under reducing conditions.

Fig. 3. Overexpression of TMPRSS11E promoted NSCLC cell proliferation and migration in vitro. A. TMPRSS11E expression in the normal lung cell line BEAS-2B and four NSCLC cell lines. A1, qRT-PCR analysis. A2, Western blot analysis. B. CCK-8 assays (A549 cells). C. Colony formation assays (A549 cells). D. TMPRSS11E promoted cell invasion and migration. A549 cells were transfected with plasmid pCMV or pCMV encoding TMPRSS11E or TMPRSS11E S372A. Representative membranes were stained with crystal violet solution. Quantitative analysis of the number of cells that migrated to the lower side of the membrane is shown. E. A wound-healing assay was used to detect A549 cell motility changes after overexpressing wild-type and mutant TMPRSS11E. *P <0.05; **P <0.01; ***P <0.001; ****P <0.0001.

Fig. 4. In vivo function of TMPRSS11E. A. Overexpression of TMPRSS11E promoted A549 cell proliferation in a xenograft tumor model. A1, tumor growth curves: intratumoral injection of TMPRSS11E-expressing plasmid promoted solid tumor growth. Each group contained 6 mice. A2, Tumor pictures. A3, Tumor weight of each group obtained 28 days after inoculation. Data represent the means ± SEMs. A4. Detection of TMPRSS11E expression in tumors transfected with plasmid. B. The effect of shTMPRSS11E plasmid transfection on the mRNA and protein levels of TMPRSS11E in 95D cells. B1, RT-PCR. B2. Western blot analysis. C. TMPRSS11E knockdown inhibited 95D cell proliferation in a

xenograft tumor model. C1, Tumor growth curves. Each group contained 6 mice. C2, Tumor pictures. C3, Tumor weight of four groups obtained 28 days after inoculation. Data represent the means \pm SEMs.

Fig. 5. STAT3 mediated TMPRSS11E transcription. A. Nucleotide sequence of the promoter region of the TMPRSS11E gene. Two STAT3-binding sites (site A and site B) were predicted. +1 indicates the position of the transcription initiation site of the TMPRSS11E gene. B. Both predicted STAT3 binding sites contributed to TMPRSS11E promoter activity. Left : Schematic diagram of the luciferase reporter constructs containing the indicated promoter fragments of the TMPRSS11E gene. The right panel shows the results of the luciferase reporter assay. A549 or 95D cells were transiently cotransfected with the indicated luciferase reporter constructs along with the pRSV- β -galactosidase plasmid. Data represent the means \pm SEMs. Mutation of site A or a short mutation of site B significantly inhibited TMPRSS11E promoter activity. C&D. The TMPRSS11E promoter was activated by STAT3. A549 cells or 95D cells were transfected with STAT3 WT (STAT3)- or STAT-3C-expressing plasmids, together with TMPRSS11E promoter constructs. Luciferase activity was detected. E. A549 cells or 95D cells were transfected with STAT3 WT plasmid or variants STAT-3C expressing plasmid, and TMPRSS11E expression levels were examined. F. Cells were transfected with STAT3 WT plasmid and then treated with increased amounts of STAT3 inhibitor BP-1-102. The TMPRSS11E expression level was examined. G. EMSA analysis. The DNA probe A (-862 to -885nt, containing the predicated STAT3 binding site A) and probe B (-517 to -541 nt, containing the predicated STAT3 binding site B) bound to the nuclear protein extracted from pCMV3-STAT3-FLAG-transfected A549 cells or 95D cells, and this binding was blocked by excess unlabeled probes. STAT3 antibody could super-shift the binding band. H. ChIP assays. STAT3 protein binding to the TMPRSS11E promoter region. Data represent the means \pm SEMs. ***P <0.001.

Fig. 6. TMPRSS11E recombinant SP protein activated PAR2. **A.** PAR2 was upregulated in NSCLC. **A1.** Expression of PAR2 in LUAD or LUSC from TCGA data. (<http://ualcan.path.uab.edu/index.html>). LUAD: Lung adenocarcinoma, LUSC: Lung squamous cell carcinoma. T: tumor; N: normal tissues. **A2.** Survival curves of the TCGA NSCLC dataset. **B.** Analysis of the enzymatic activity of the human TMPRSS11E protease domain on synthetic IQF peptide substrates. (The IQF sequence was the PAR2 N-terminal peptide 33SKGRSLIG40, which contains the PAR2 activation site). **B1.** TMPRSS11E SP cleavage of IQF peptides was detected by monitoring the fluorescence signal. Purified recombinant TMPRSS11E or trypsin was incubated with 50 μ M chromogenic peptide substrate at 37 °C for 15 min, and the fluorescence released was monitored. **B2.** The kinetic parameter of TMPRSS11E for the substrate was determined using the standard Michaelis–Menten equation. Measurements were performed in duplicate and represent the means \pm SDs of at least three independent experiments. **C.** PAR2 AP or TMPRSS11E SP protein incubation upregulated phosphorylated EGFR and STAT3 levels, while PAR2 inhibitor AZ3451 treatment reversed the effect of re-SP.

Fig.1

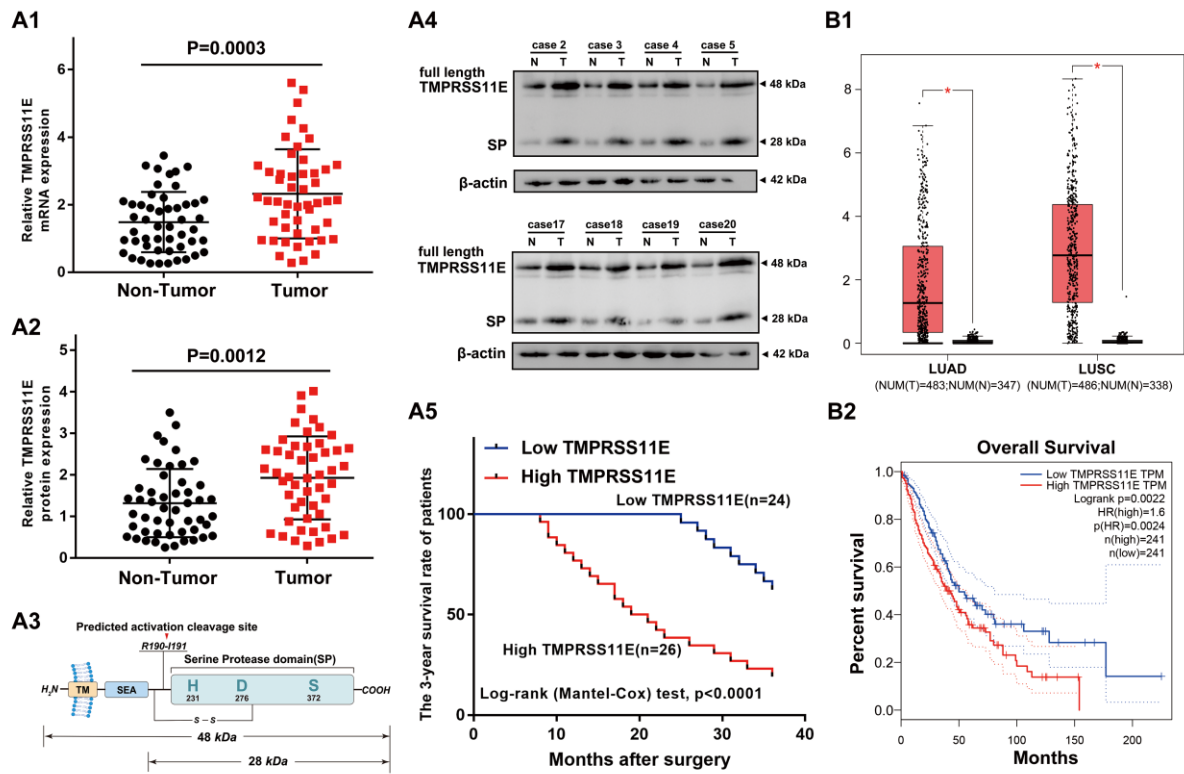


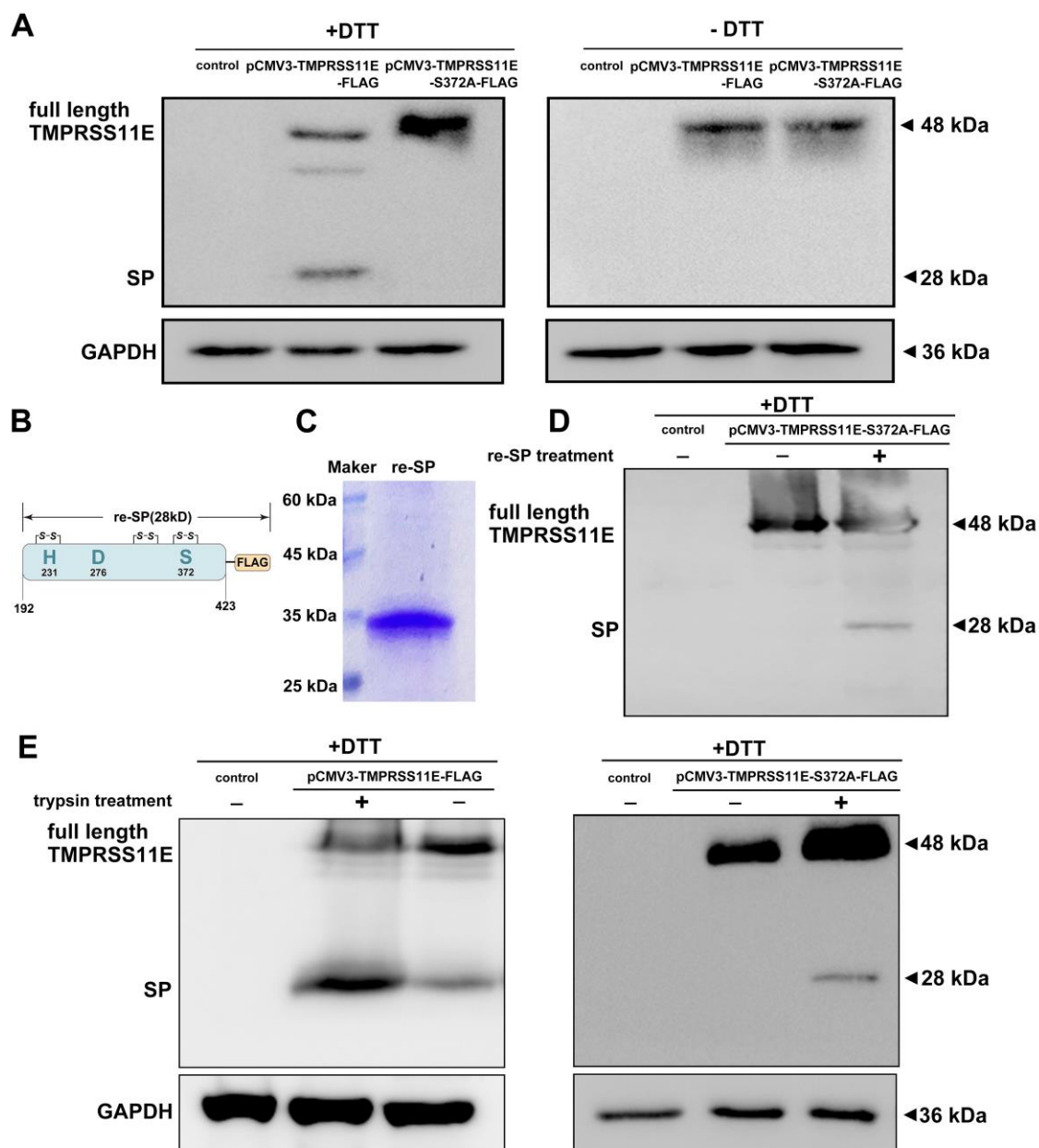
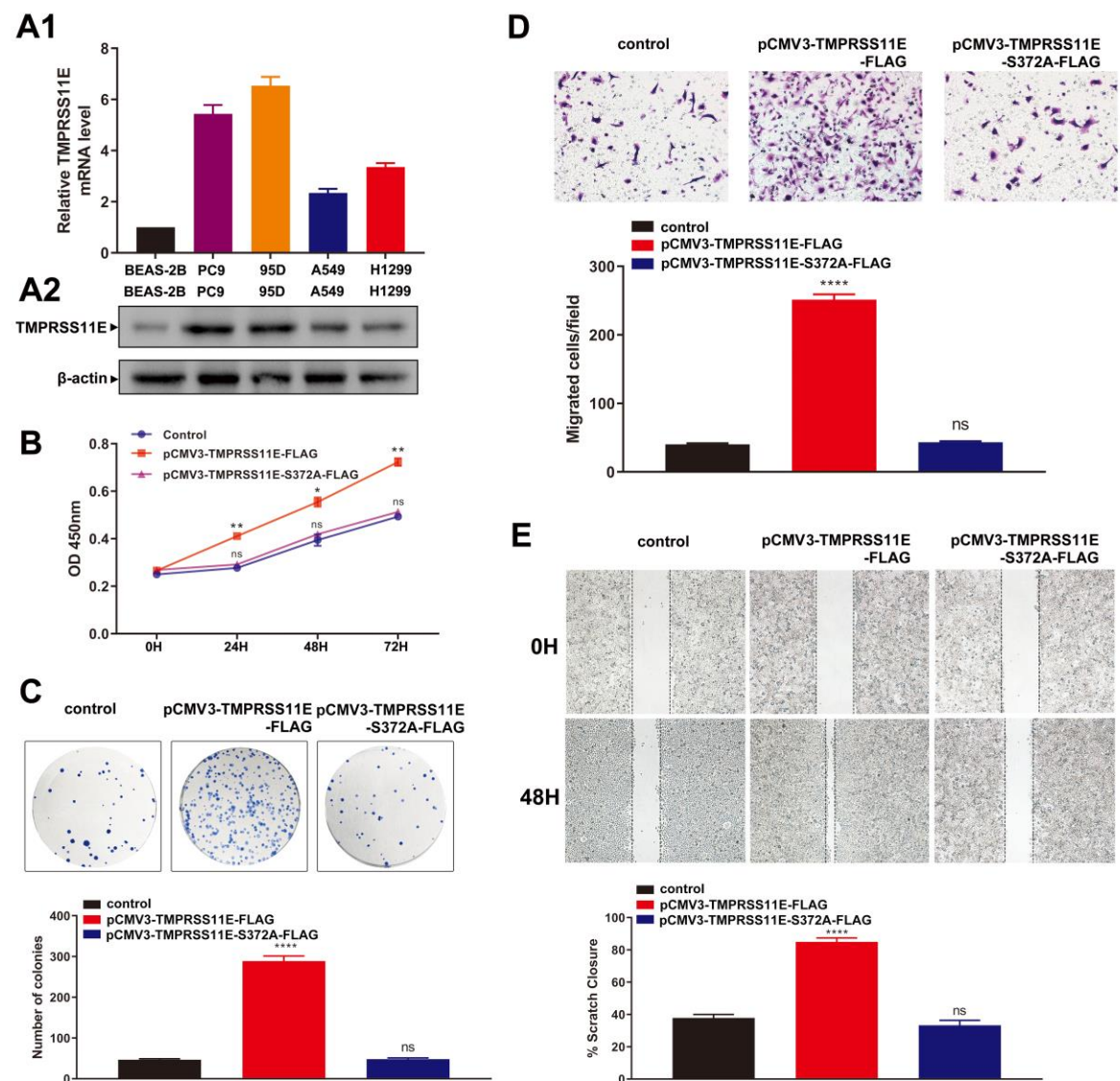
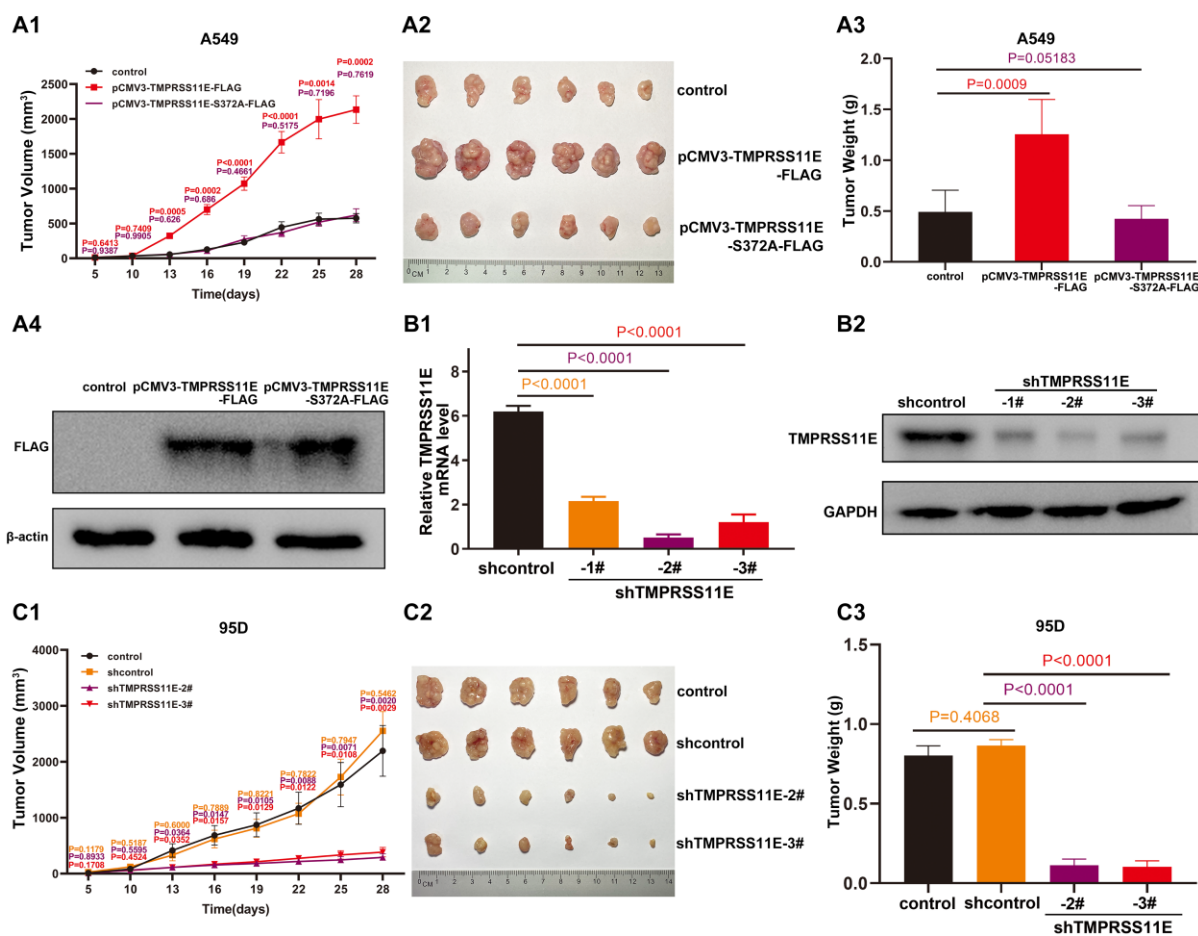
Fig.2

Fig.3



Accer

Fig.4

Accepte

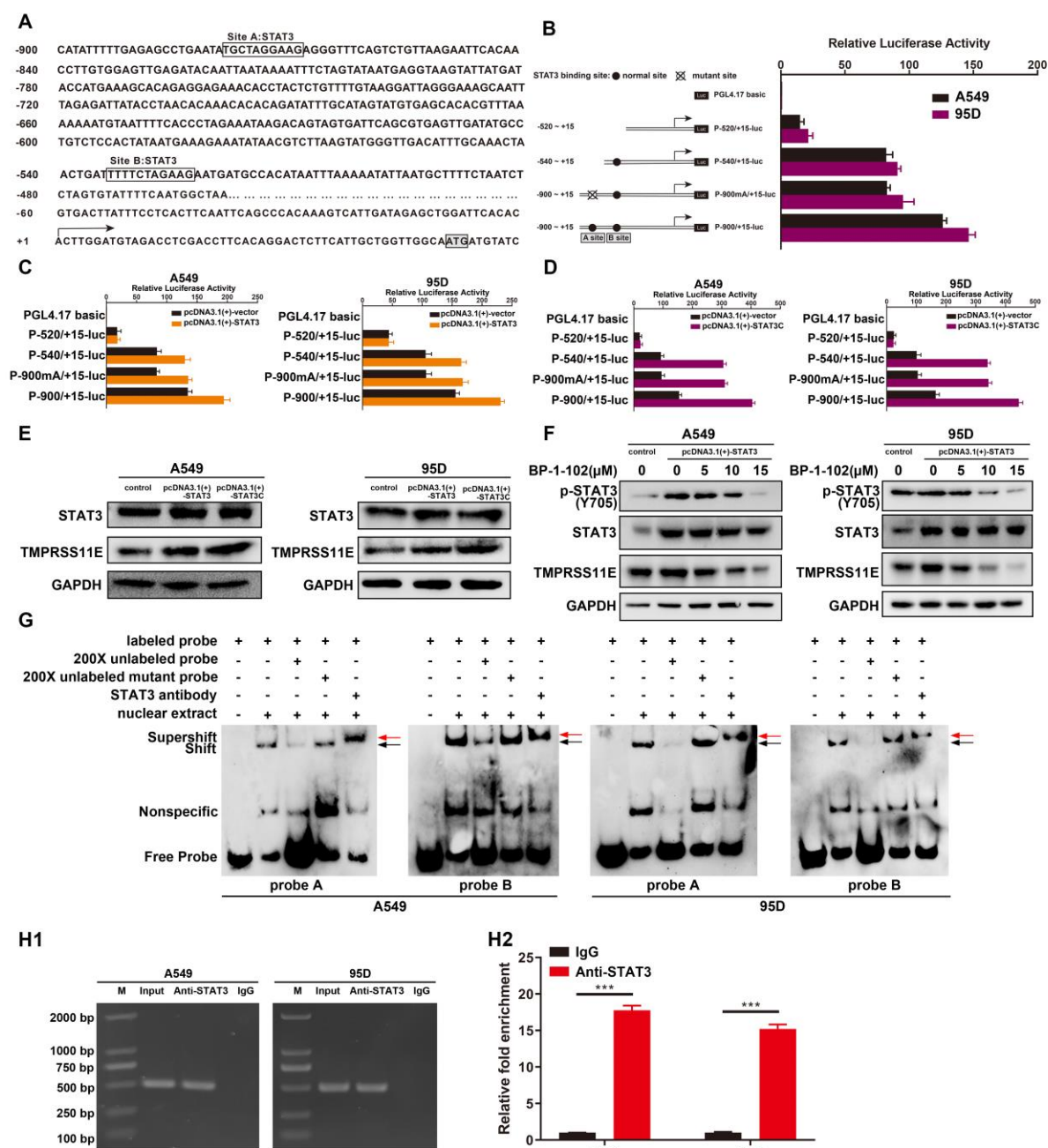
Fig.5

Fig.6

